The post-stishovite phase transition in hydrous alumina-bearing SiO$_2$ in the lower mantle of the earth

Dmitry L. Lakshtanov*[†], Stanislav V. Sinogeikin*[‡], Konstantin D. Litasov[§], Vitali B. Prakapenka[¶], Holger Hellwig*, Jingyun Wang*, Carmen Sanches-Valle*, Jean-Philippe Perrillat*, Bin Chen*, Maddury Somayazulu[∥], Jie Li*, Eiji Ohtani[§], and Jay D. Bass*

*Department of Geology, University of Illinois at Urbana–Champaign, 1301 West Green Street, Urbana, IL 61801; [§]Institute of Mineralogy, Petrology, and Economic Geology, Tohoku University, Aza Aoba Aramaki, Sendai 980-8578, Japan; [¶]GeoSoilEnviroCARS, Center for Advanced Radiation Sources, University of Chicago, Chicago, IL 60637; and [∥]Carnegie Institution of Washington, Geophysical Laboratory, 5251 Broad Branch Road NW, Washington, DC 20015

Silica is the most abundant oxide component in the Earth mantle by weight, and stishovite, the rutile-structured (P4$_2$/mnm) high-pressure phase with silica in six coordination by oxygen, is one of the main constituents of the basaltic layer of subducting slabs. It may also be present as a free phase in the lower mantle and at the core–mantle boundary. Pure stishovite undergoes a displacive phase transition to the CaCl$_2$ structure (Pnnm) at ≈55 GPa. Theory suggests that this transition is associated with softening of the shear modulus that could provide a significant seismic signature, but none has ever been observed in the Earth. However, stishovite in natural rocks is expected to contain up to 5 wt % Al$_2$O$_3$ and possibly water. Here we report the acoustic velocities, densities, and Raman frequencies of aluminum- and hydrogen-bearing stishovite with a composition close to that expected in the Earth mantle at pressures up to 43.8(3) GPa [where (3) indicates an uncertainty of 0.3 GPa]. The post-stishovite phase transition occurs at 24.3(5) GPa (at 298 K), far lower than for pure silica at 50–60 GPa. Our results suggest that the rutile–CaCl$_2$ transition in natural stishovite (with 5 wt % Al$_2$O$_3$) should occur at ≈30 GPa or ≈1,000-km depth at mantle temperatures. The major changes in elastic properties across this transition could make it visible in seismic profiles and may be responsible for seismic reflectors observed at 1,000- to 1,400-km depth.

hydrogen | phase transition | silica | high pressure | Brillouin scattering

Stishovite is the lowest-pressure SiO$_2$ polymorph with octahedrally coordinated silicon. It adopts the tetragonal rutile structure (P4$_2$/mnm) and is stable from ≈9 GPa to ≈50 GPa at room temperature where it undergoes a displacive phase transition to the orthorhombic CaCl$_2$ structure (Pnnm), e.g. (1, 2). Estimates for the temperature dependence of this transition (dP/dT) (1, 3, 4) suggested that it might occur at depths of ≈1,500 km or more in the mantle (more than ≈60 GPa), but the expected seismic signatures have never been observed in that depth range. In fact, the phase relations for pure SiO$_2$ may not be directly relevant to the mantle because they do not include the possible effects of Al$_2$O$_3$ and H$_2$O, which are known to be soluble in stishovite (5, 6). It was previously speculated that impurities might lower the pressure for this transition (7), but clear experimental evidence was lacking. If these effects are significant, they may bring the depth of this phase transition into the region where it could possibly explain seismic reflections observed at 900- to 1,400-km depth (8–11).

Results

Fig. 1 shows the angle-dispersive x-ray spectra of the stishovite and post-stishovite (CaCl$_2$) polymorphs. Because these single-crystal x-ray diffraction (XRD) spectra were obtained by a rotation of only ±12° on the ω-circle, not all reflections are present. However, the CaCl$_2$ phase was clearly observed on our x-ray spectra above 24 GPa. The volume change of transition is apparently small (12), and the tetragonal–orthorhombic symmetry change can be difficult to resolve. This limitation is a common one among XRD methods of detecting displacive phase transitions, sometimes leading to an uncertainty of >10 GPa in the transition pressure, P$_{tr}$ (13, 14). Here, the MAR-345 images (Fig. 1) clearly show splitting of the (121) and (211) peaks for the orthorhombic higher-pressure phase at 24.8(3) GPa.

Brillouin scattering measurements were performed from nearly the same scattering volume that was probed in the XRD measurements. The orientation of the sample allowed us to collect acoustic velocities close to the [110] phonon direction. In this direction, the elastic shear modulus $V_{S_H}^2 \rho = C_{11} - C_{12}$ should vanish approaching P$_{tr}$ (15). Our Brillouin sound velocity measurements show softening of this acoustic mode (Fig. 2), allowing us to bracket the pressure of the phase transition between 20.0(3) and 24.8(3) GPa. In the lower-symmetry CaCl$_2$ phase, dV_{S_H}/dP is larger by the nature of the transition, hence the P$_{tr}$ should be located at a pressure closer to 24.8(3) GPa.

Raman scattering results obtained on pressure decrease (Fig. 2) help to refine further the pressure of the transition. The softening of the mode B$_{1g}$ in the rutile structure is clearly followed by a stiffening of the A$_g$ mode in the CaCl$_2$ structure. The intersection of linear least-squares fits to the squares of the mode frequencies provides us with a transition pressure P$_{tr}$ = 24.3(3) GPa (15, 16).

Discussion

The post-stishovite phase transition in pure SiO$_2$ is thought to occur at 50–60 GPa (1, 2, 15, 17). The enormous decrease of transition pressure in aluminous stishovite (which to some extent can be considered a SiO$_2$-δAlOOH solid solution) (18), compared with the pure end-member, and the pronounced acoustic mode softening documented in our work, opens the possibility of a signature of this phase transition in the upper part of the lower mantle. Our results should be more directly applicable to the Earth mantle because the Al$_2$O$_3$ content of natural stishovite in chemically complex mantle assemblages may be as high as 5 wt % (19, 20). If we assume a linear dependence of the transition pressure on aluminum content, $dP_{tr}/dX_{Al_2O_3}$ (Fig. 3), and a Clapeyron slope, $dP_{tr}/dT = 0.004$ GPa/K(1), we estimate a lower bound of $P ≈36$ GPa for the pressure at which this phase transition would occur in the mantle, corresponding to a depth of ≈1,000 km.

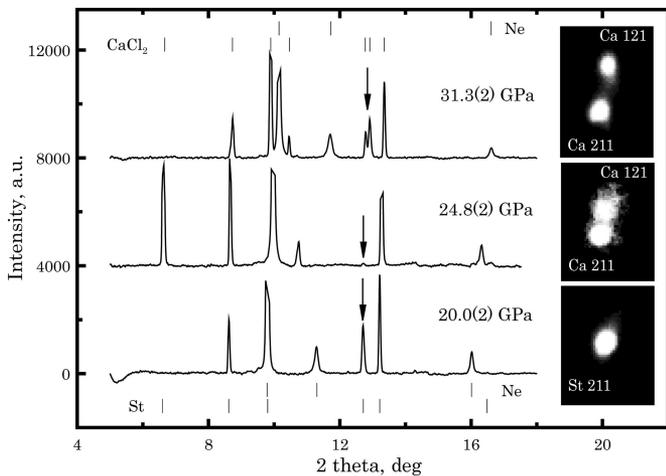**Fig. 1.** Angle dispersive x-ray spectra of aluminous stishovite K324 across the rutile ↔ CaCl$_2$ phase transition. Positions for the most intense stishovite (St), CaCl$_2$ phase (Ca), and neon (Ne) peaks are marked with vertical bars. MAR345 2D images at the right correspond to the peaks marked on the spectra by down-pointing arrows.

There have been numerous reports of seismic discontinuities and heterogeneities in the depth range of 1,000–1,500 km (8–10). Kaneshima and Helffrich (8) and Niu *et al.* (11) found a dipping low-velocity layers (LVL) in the vicinity of the Mariana and Izu–Bonin subduction zones, and they estimated the thickness of the LVL to be ≈8 km (8) to ≈12 km (11), with a shear velocity anomaly of 2–6%. These authors ruled out a phase transition source for the LVL because of the dipping nature of the anomaly. However, shear softening related to the rutile–CaCl$_2$ transition in aluminous stishovite within the mid-ocean ridge basalts (MORB) part of a subducted slab may provide a viable explanation for this feature. Similarly, LeStunff *et al.* (9) observed a reflector at ≈1,200 km in a rather different tectonic setting, under the African Rift zone. They concluded that a sharp (<20–25 km thick) feature was responsible for the reflection of low-frequency $P'P'$ precursors. Only a few vol % of stishovite is
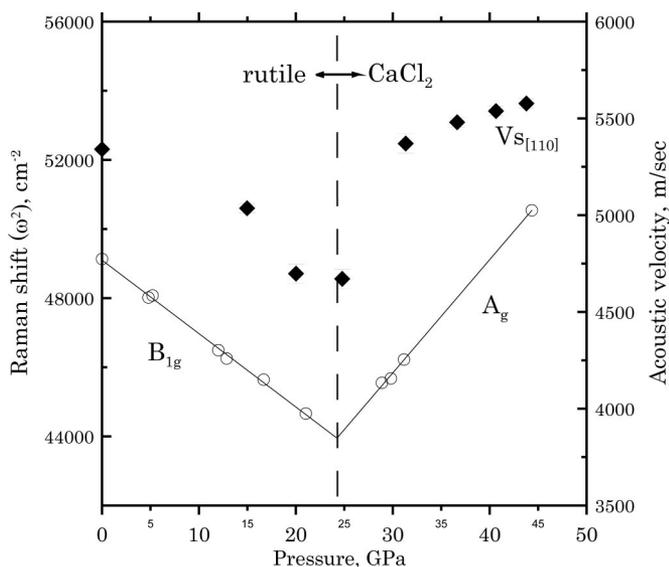

Fig. 2. Acoustic velocities (solid symbols) and squares of the Raman frequencies (open symbols) across the rutile–CaCl$_2$ phase transition in K324 stishovite. Solid line, linear fit to square of the Raman frequencies; dashed line, P_{tr} derived from the Raman data.
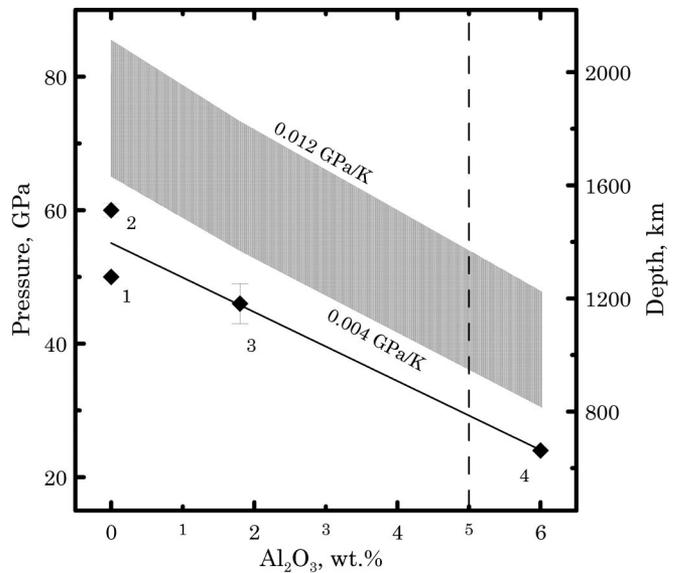

Fig. 3. Pressure of the rutile–CaCl$_2$ P_{tr} as a function of Al$_2$O$_3$ content. 1, from ref. 1; 2, from ref. 13; 3, from ref. 7; 4, this work. Shaded region shows the range of P_{tr} at mantle PT conditions, with the lower bound of dP_{tr}/dT from (1) and upper bound from (4). Solid line, linear fit to experimental points; dashed line, maximum Al$_2$O$_3$ content observed in natural systems (19).

needed to cause a visible seismic discontinuity (21), whereas stishovite may comprise up to ≈20 vol % of subducted MORB material.

Previously, stishovite had been considered to be an explanation of these reflectors (1, 15), but it appeared that the transition would occur too deep in the lower mantle (4). Our observations show that seismic reflectors in the depth interval of ≈1,000–1,500 km may be the signature of subducted MORB material not only in the regions of active subduction (8), but also in the regions where subduction became extinct in Mesozoic or even Proterozoic (9). On the other hand, some authors have argued for the existence of stishovite in "ambient" lower-mantle lithologies (22–25). Although it appears likely that the bulk of the lower mantle is dominated by magnesian silicate perovskite and ferropericlase, the possibility of stishovite (rutile or CaCl$_2$-structured) occurring locally in lower mantle chemical heterogeneities may explain the spatially restricted character of seismic reflectors in this depth interval.

Natural occurrences of stishovite are largely restricted to meteorites and impact craters. In studies of impacts, stishovite serves as an important pressure marker. However, sometimes, as in case of the Shergotty meteorite, there is a mismatch between the observed phase assemblages and the pressure deduced from such markers e.g., refs. 26 and 27. Chemical analyses of stishovite from the Shergotty meteorite show that it contains >1.5 wt % impurities such as Na$_2$O and Al$_2$O$_3$. Our results show that aluminum and possibly hydrogen have a large effect on the stability fields of silica phases. Thus, careful chemical analysis of quenched phases and consideration of the effect of minor elements on phase boundaries are required for an accurate determination of peak pressure in shocked assemblages.

Materials and Methods

The sample studied in this work [K324, containing 6.07(5) wt % Al$_2$O$_3$ and 0.24(2) wt % H$_2$O synthesized at 20 GPa and 1,800°C (28)] was a single-crystal plate with the normal to the surfaces having direction cosines of (−0.603 0.522 0.603). The ambient-pressure elastic properties and Raman frequencies of this and other crystals from the same batch were reported elsewhere (28).

The crystal was loaded into a symmetric piston-cylinder diamond-anvil cell along with four ruby spheres (29) and two chips of NaCl. Neon served as a pressure-transmitting medium because it provides quasi-hydrostatic conditions to pressures >60 GPa (1, 30). The choice of pressure medium was important because displacive phase transitions are sensitive to nonhydrostatic stress (15, 31).

Simultaneous Brillouin scattering and synchrotron XRD measurements were performed at 13-BMD, GeoSoilEnviroCARS, Advanced Phonon Source (Argonne, IL). We used the recently developed Brillouin scattering system (32) and angle-dispersive x-ray diffraction with an MAR-345 (Mar-USA, Evanston, IL) imaging plate detector. Pressure was increased in small (<1 GPa) increments with a typical spacing of ≈5 GPa between Brillouin measurements. After each pressure increase above 20 GPa, the cell was annealed in an oven at 200–300°C for 0.5–24 h or laser-heated at ≈1,500°C (CO_2 laser, $\lambda = 10 \mu m$) to relax deviatoric stresses in the sample chamber. The pressure gradient never exceeded 0.5 GPa in any experiment, as monitored by x-ray diffraction from the pressure medium (neon) and ruby fluorescence.

Raman scattering measurements obtained on decreasing pressure were performed at the University of Illinois. At pressures of 38.4(7) and 28.7(3) GPa, the pressure medium was annealed at 300°C for 30 min.

1. Kingma KJ, Cohen RE, Hemley RJ, Mao HK (1995) *Nature* 374:243–245.
2. Andrault D, Fiquet G, Guyot F, Hanfland M (1998) *Science* 282:720–724.
3. Tsuchiya T, Caracas R, Tsuchiya J (2004) *Geophys Res Lett* 31:art no L11610.
4. Ono S, Hirose K, Murakami M, Isshiki M (2002) *Earth Planet Sci Lett* 197:187–192.
5. Pawley AR, Mcmillan PF, Holloway JR (1993) *Science* 261:1024–1026.
6. Chung JI, Kagi H (2002) *Geophys Res Lett* 29:art no 2020.
7. Lakshtanov DL, Vanpeteghem CB, Jackson JM, Bass JD, Shen GY, Prakapenka VB, Litasov K, Ohtani E (2005) *Phys Chem Miner* 32:466–470.
8. Kaneshima S, Helffrich G (1999) *Science* 283:1888–1891.
9. LeStunff Y, Wicks CW, Jr, Romanowicz B (1995) *Science* 270:74–77.
10. Kawakatsu H, Niu FL (1994) *Nature* 371:301–305.
11. Niu FL, Kawakatsu H, Fukao Y (2003) *J Geophys Res-Solid Earth* 108:art no 2419.
12. Hemley RJ, Shu J, Carpenter MA, Hu J, Mao HK, Kingma KJ (2000) *Solid State Commun* 114:527–532.
13. Andrault D, Angel RJ, Mosenfelder JL, Le Bihan T (2003) *Am Mineral* 88:301–307.
14. Shim SH, Jeanloz R, Duffy TS (2002) *Geophys Res Lett* 29:art no 2166.
15. Carpenter MA, Hemley RJ, Mao HK (2000) *J Geophys Res Solid Earth* 105:10807–10816.
16. Dove MT (1993) *Introduction to Lattice Dynamics* (Cambridge Univ Press, New York).
17. Cohen RE (1992) in *High Pressure Research*: *Applications to Earth and Planetary Sciences*, ed. Syono Y, Manghnani MH (American Geophysical Union, Washington, DC), pp 425–432.
18. Panero WR, Stixrude LP (2004) *Earth Planet Sci Lett* 221:421–431.
19. Irifune T, Ringwood AE (1993) *Earth Planet Sci Lett* 117:101–110.
20. Litasov K, Ohtani E (2006) *Physics Earth Planetary Interiors* 150:239–263.
21. Karki BB, Stixrude L, Crain J (1997) *Geophys Res Lett* 24:3269–3272.
22. Saxena SK, Dubrovinsky LS, Lazor P, Cerenius Y, Haggkvist P, Hanfland M, Hu JZ (1996) *Science* 274:1357–1359.
23. Meade C, Mao HK, Hu JZ (1995) *Science* 268:1743–1745.
24. Knittle E, Jeanloz R (1986) *Geophys Res Lett* 13:1541–1544.
25. Stixrude L, Bukowinski MST (1992) *Geophys Res Lett* 19:1057–1060.
26. Sharp TG, El Goresy A, Wopenka B, Chen M (1999) *Science* 284:1511–1513.
27. El Goresy A, Dubrovinsky L, Sharp TG, Chen M (2004) *J Phys Chem Solids* 65:1597–1608.
28. Lakshtanov DL, Litasov KD, Sinogeikin SV, Hellwig H, Li J, Ohtani E, Bass JD (2007) *Am Mineral* 92:1026–1030.
29. Chervin JC, Canny B, Mancinelli M (2002) *High Pressure Res* 21:305–314.
30. Hemley RJ, Zha CS, Jephcoat AP, Mao HK, Finger LW, Cox DE (1989) *Phys Rev B* 39:11820–11827.
31. Dubrovinsky LS, Belonoshko AB (1996) *Geochim Cosmochim Acta* 60:3657–3663.
32. Sinogeikin S, Bass J, Prakapenka V, Lakshtanov D, Shen GY, Sanchez-Valle C, Rivers M (2006) *Rev Sci Instrum* 77:1–11.